

**Metallization of aluminum hydride at high pressures: A first-principles study**

Chris J. Pickard

*Scottish Universities Physics Alliance, School of Physics and Astronomy, University of St Andrews, St Andrews, KY16 9SS, United Kingdom*

R. J. Needs

*Theory of Condensed Matter Group, Cavendish Laboratory, Cambridge CB3 0HE, United Kingdom*

(Received 19 July 2007; published 29 October 2007)

We have used first-principles density-functional-theory electronic structure methods and a random searching technique to identify stable high pressure phases of aluminum hydride ( $\text{AlH}_3$ ). We find a transition from the insulating low-pressure  $\alpha$  phase to an insulating layered structure of space group  $Pnma$  at 34 GPa, and a transition to a semimetallic  $Pm\bar{3}n$  phase at 73 GPa. These phases are predicted to be stable against dehydrogenation (the evolution of  $\text{H}_2$  molecules), and they could be formed at pressures easily attainable within diamond-anvil-cell experiments.

DOI: [10.1103/PhysRevB.76.144114](https://doi.org/10.1103/PhysRevB.76.144114)

PACS number(s): 62.50.+p, 71.15.Nc, 71.20.-b, 74.62.Fj

**I. INTRODUCTION**

Aluminum hydride (or alane,  $\text{AlH}_3$ ) is a solid with a very large hydrogen content of 10.1% by weight. It has been proposed as a material for storing hydrogen in hydrogen-fueled vehicles, although there is currently no commercially viable process for turning the spent Al powder back into  $\text{AlH}_3$ .<sup>1</sup> Aluminum hydride is also a promising additive to rocket fuels and high explosives.<sup>2</sup>

The large hydrogen content which is important for hydrogen storage can also lead to other interesting properties. Stable materials containing large fractions of H atoms tend to be insulators at low pressures because it is energetically favorable for them to form filled-shell electronic configurations. However, all materials are expected to metallize at sufficiently high pressures, and recently there has been interest in compressed hydrides as possible high-temperature superconductors. Materials containing a large fraction of H atoms are promising for this purpose because the small mass of the proton leads to very high Debye temperatures which, according to the standard Bardeen-Cooper-Schrieffer (BCS) theory,<sup>3</sup> promotes superconductivity. Metallization of pure hydrogen appears to be beyond the reach of current high pressure cells, but hydrides might metallize at considerably lower pressures.<sup>4</sup> Theoretical<sup>5-7</sup> and experimental<sup>8</sup> studies of silane ( $\text{SiH}_4$ ), and theoretical studies of germane<sup>9</sup> ( $\text{GeH}_4$ ) and stannane<sup>10</sup> ( $\text{SnH}_4$ ), have investigated possible metallization at high pressures. The results obtained are sufficiently encouraging to prompt studies of a wider range of hydrides.

In reviewing the known properties of binary hydrides our attention was drawn to aluminum hydride which contains a large fraction (3/4) of H atoms and is readily available for experimental studies. The Pauling electronegativities (Al: 1.61, H: 2.20) are such that electronic charge is transferred from the Al to the H atoms, and the occupied electronic states at zero pressure are strongly associated with the H atoms. As  $\text{AlH}_3$  has two valence electrons per H atom, the H-derived bands are filled at low pressures, and aluminum hydride is an insulator. At high pressures the atoms are forced closer together and the ionicity of the bonding is de-

creased. If this effect is sufficient to transfer significant charge onto the Al atoms then a metallic phase will be formed. The relatively large electronic charge on the H atoms also enhances the possibility of strong electron-phonon coupling related to motion of the H atoms, which could promote high temperature superconductivity. We therefore decided to search for high-pressure phases of aluminum hydride, hoping to find a stable metallic phase at reasonably low pressures.

The structures of four different low-pressure insulating polymorphs of aluminum hydride or aluminum deuteride have been determined experimentally, the  $\alpha$ ,<sup>11</sup>  $\alpha'$ ,<sup>11</sup>  $\beta$ ,<sup>12</sup> and  $\gamma$  (Ref. 13) phases, with the  $\alpha$  phase being the most stable at standard temperature and pressure (STP). Other polymorphs have been reported, such as the  $\delta$  and  $\epsilon$  phases, but these may be related to the presence of impurities.<sup>12</sup>

Ke *et al.*<sup>14</sup> studied the low-pressure phases of  $\text{AlH}_3$  using first-principles density functional theory (DFT) calculations. Graetz *et al.*<sup>15</sup> used such methods to study  $\alpha$ - $\text{AlH}_3$ , finding that it remains insulating up to at least 100 GPa. We are not, however, aware of any DFT studies of other possible high-pressure structures of  $\text{AlH}_3$ .

**II. RANDOM STRUCTURE SEARCHING**

We have studied high-pressure phases of  $\text{AlH}_3$  using first-principles DFT methods and the “random searching” technique used in earlier projects on silane,<sup>6</sup> graphite intercalation compounds,<sup>16</sup> and hydrogen.<sup>17</sup> We create a set of initial structures by choosing random unit cells, renormalizing the volume to a reasonable value, and inserting the desired number and types of atoms at random positions within the cell. Each of these structures is then relaxed to a minimum in the enthalpy at fixed pressure. New random structures are generated and relaxed until the most stable ones are obtained several times. Searches are then repeated for different numbers of  $\text{AlH}_3$  formula units per cell. This simple algorithm has the appealing features that it does not involve the choice of highly system-specific parameters and it is largely unbi-

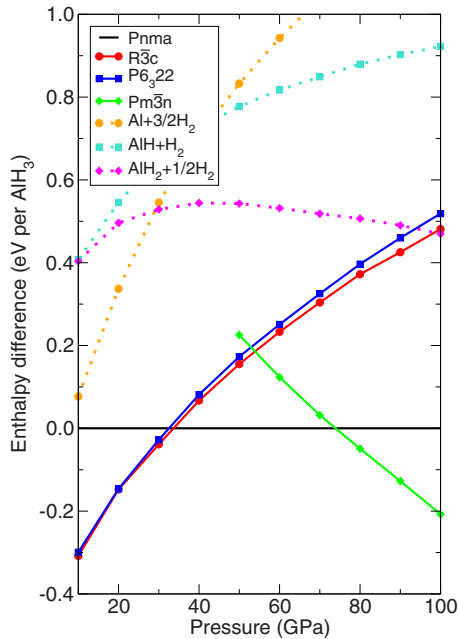


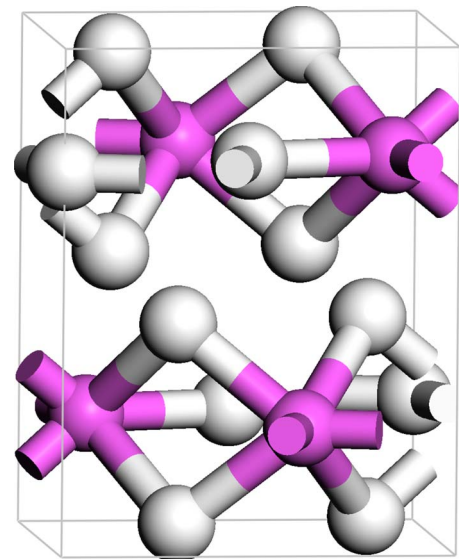
FIG. 1. (Color online) Enthalpy per  $\text{AlH}_3$  unit as a function of pressure for the low enthalpy phases found in the structure search. The dotted lines indicate dehydration into Al, AlH, or  $\text{AlH}_2$ , and  $\text{H}_2$ .

ased towards a particular type of inter-atomic bonding or structure.

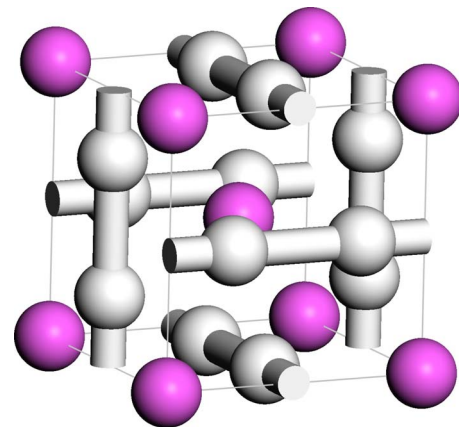
Our calculations were performed using the CASTEP plane-wave code,<sup>18</sup> the Perdew-Burke-Ernzerhof (PBE) generalized gradient approximation (GGA) density functional,<sup>19</sup> and ultrasoft pseudopotentials.<sup>20</sup> We use a plane wave cutoff of 230 eV and a Brillouin zone sampling grid spacing of  $2\pi \times 0.07 \text{ \AA}^{-1}$  for the searches, and 260 eV and  $2\pi \times 0.04 \text{ \AA}^{-1}$  for subsequent calculations. Extensive random searches were performed at pressures of 10, 50, and 100 GPa, using unit cells containing 3 and 4 formula units. We then selected the lower enthalpy phases and recalculated their enthalpies at a larger number of pressures, generating the data shown in Fig. 1.

### III. RESULTS FROM STRUCTURE SEARCHING

The searches at 10 GPa produced the insulating  $\alpha$  phase several times (without the slight monoclinic distortion suggested by Graetz *et al.*<sup>15</sup>), which is believed to be the most stable phase at low pressures. The  $\alpha$  phase has space group symmetry  $R\bar{3}c$ , and consists of corner-shared  $\text{AlH}_6$  octahedra. A structure of symmetry  $P6_322$  was also found, which is related to the  $R\bar{3}c$  structure. In the pressure range 34–73 GPa an insulating layered structure of space group  $Pnma$  was most stable, shown in Fig. 2 with the parameters given in Table I. This structure has the same symmetry as the cementite phase of  $\text{Fe}_3\text{C}$ , although the parameters are such that it is more layerlike in  $\text{AlH}_3$ . The bonding in both the  $R\bar{3}c$  and  $Pnma$  structures consists of H bridges between neighboring Al atoms. In  $R\bar{3}c$  each pair of Al atoms is



(a)



(b)

FIG. 2. (Color online) The structures of the  $Pnma$  phase at 50 GPa (top), and the  $Pm\bar{3}n$  phase at 80 GPa (bottom). The Al atoms are shown as dark spheres and the H atoms as light spheres. For both structures, bonds have been drawn between atoms separated by less than  $1.75 \text{ \AA}$ . The layers and the Al-H-Al bridges of the  $Pnma$  phase are clearly visible. The H chains and body-centered cubic lattice of Al atoms of the  $Pm\bar{3}n$  can also be seen.

bridged by a single H atom, while in  $Pnma$  there are both single and double bridges, so that this structure contains two inequivalent H positions.

At 73 GPa, a phase of space group  $Pm\bar{3}n$  becomes favorable. The  $Pm\bar{3}n$  structure is illustrated in Fig. 2, and its parameters are given in Table I. This structure is of very high symmetry, consisting of a body-centered-cubic array of Al atoms and chains of equivalent H atoms along each Cartesian direction, with a primitive unit cell containing two formula units. The  $Pm\bar{3}n$  structure is, in fact, the same as that of the superconductor  $\text{Nb}_3\text{Sn}$  (niobium stannide), which is used in applications where high magnetic fields are present, such as magnetic resonance imaging (MRI) scanners, particle accelerators, and nuclear fusion research.

TABLE I. The structures of the  $Pnma$  and  $Pm\bar{3}n$  phases.

Pressure (GPa)	Space group	Lattice parameters ( $\text{\AA}$ , deg.)			Atomic coordinates (fractional)			
		$a$	$b$	$c$				
50	$Pnma$	$a=4.083$	$b=5.259$	$c=3.593$	Al	0.1104	0.2500	0.5330
		$\alpha=90.00$	$\beta=90.00$	$\gamma=90.00$	H1	0.3090	0.4458	0.8400
					H2	0.4879	0.2500	0.3924
80	$Pm\bar{3}n$	$a=3.169$	$b=3.169$	$c=3.169$	Al	0.0000	0.0000	0.0000
		$\alpha=90.00$	$\beta=90.00$	$\gamma=90.00$	H	0.2500	0.0000	0.5000

#### IV. ELECTRONIC STRUCTURE OF THE PHASES

The band gap of the  $R\bar{3}c$  phase was calculated to be 2.45 eV at zero pressure. However, it is well known that standard density functionals, such as the PBE-GGA, tend to underestimate band gaps, and a recent  $GW$  many-body perturbation theory calculation<sup>21</sup> gave a larger band gap of 3.54 eV.<sup>22</sup> Because of the expected underestimation of the band gap in PBE-GGA, we also performed band structure calculations using the screened exchange (sX) local density approximation (LDA) functional which, for  $sp$ -bonded semiconductors, gives band gaps in substantially better agreement with experiment.<sup>23</sup> Using the sX-LDA increases the band gap of  $R\bar{3}c$  by 0.9 eV, leading to good agreement with the  $GW$  value.  $Pnma$  is also found to be an insulator, even at high pressures, with a PBE-GGA band gap of 2.07 eV at 80 GPa, see Fig. 3.

The band structure of  $Pm\bar{3}n$   $\text{AlH}_3$  at 80 GPa is shown in Fig. 4. The PBE-GGA calculations give an indirect band gap overlap of about 1.5 eV at 80 GPa which, unusually, de-

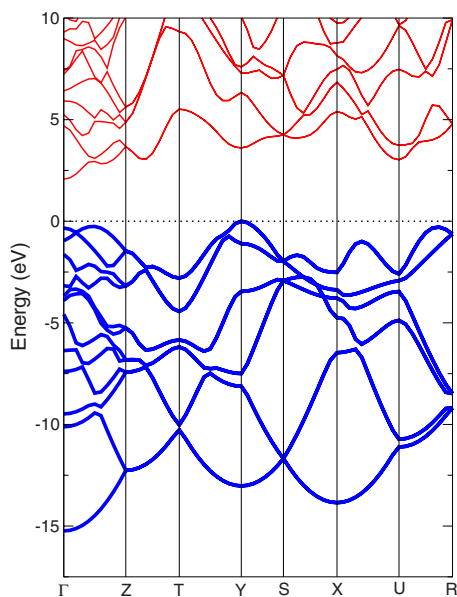


FIG. 3. (Color online) Band structure of the  $Pnma$  phase of  $\text{AlH}_3$  at 80 GPa, calculated at the PBE-GGA level. The thick lines indicate the H-derived electronic bands, and the thin lines indicate the mainly Al-derived bands. The bands with energies below zero are occupied, and the higher energy bands are unoccupied.

creases (very slowly) with increasing pressure, although our calculations suggest that this phase remains metallic at higher pressures, at least up to 300 GPa. The band minimum near the Fermi level at the  $R$  point is a highly dispersive state associated with the Al atoms. The band maximum at the  $M$  point is associated with the chains of H atoms, and exhibits substantial energy overlap with the Al-derived band at  $R$ . The Fermi surface of  $Pm\bar{3}n$  therefore contains electronic states of very different character. The calculated density of states at the Fermi level is about 1/4 of that of the free electron gas at the same average electron density. Our sX-LDA calculations show that  $Pm\bar{3}n$  remains metallic at this level of description, reducing the band overlap by 0.36 eV at 80 GPa. Figure 5 shows that the density of states at the Fermi level of the  $Pm\bar{3}n$  structure is quite small and the material might best be described as a semimetal.

The total electronic charge density of the  $Pm\bar{3}n$  phase, and the charge densities of an H-derived state and an Al-derived state are illustrated in Fig. 6. The total charge density

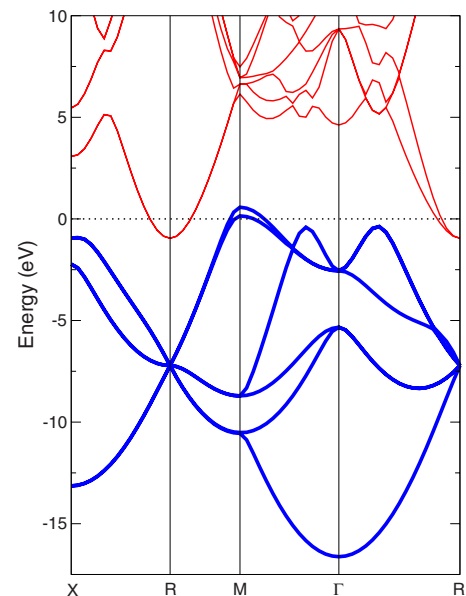


FIG. 4. (Color online) Band structure of the  $Pm\bar{3}n$  phase of  $\text{AlH}_3$  at 80 GPa, calculated at the PBE-GGA level. The thick lines indicate the H-derived electronic bands, and the thin lines indicate more diffuse, mainly Al-derived, bands. The Fermi level is at zero energy, so that the H-derived states near  $M$  are unoccupied, while the mainly Al-derived states at  $R$  are occupied.

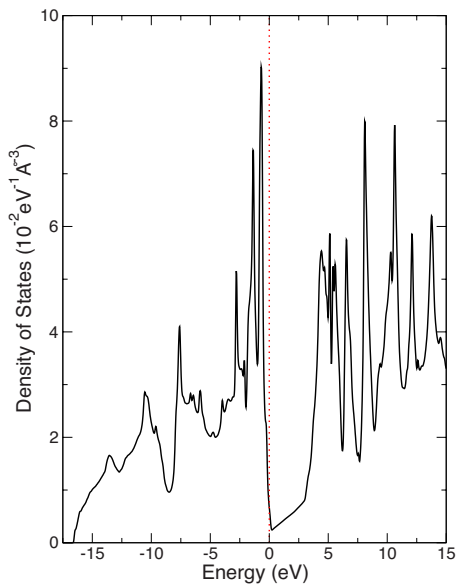


FIG. 5. (Color online) The electronic density of states of the  $Pm\bar{3}n$  phase of  $AlH_3$  at 80 GPa. The Fermi energy is shown as a dotted vertical line at zero energy.

shows strong ionic bonding, with almost complete charge transfer from the Al to the H atoms. The density of the (unoccupied) electronic state at the  $M$  point shown in Fig. 6 is similar to the total density, but the charge density from the (occupied) electronic state at the  $R$  point in Fig. 6 is mainly on the Al atoms. There is a tendency for the ionicity of materials to decrease at smaller volumes. At 80 GPa, the volume of the  $Pm\bar{3}n$  structure is 8% smaller than that of  $Pnma$ . The smaller volume gives greater spatial overlap of the orbitals on neighboring atoms, which leads to greater band dispersion and to energy overlap between the H and Al derived bands. This reduces the ionicity and leads to the semimetallic behavior of the  $Pm\bar{3}n$  phase.

We performed DFT calculations of phonon frequencies of the  $Pm\bar{3}n$  structure at 80 GPa. Using the highest calculated phonon frequency as a measure of the Debye frequency, we obtained a Debye temperature of 2700 K, which would tend to favour superconductivity, but the total density of electronic states at the Fermi energy is not very large, which militates strongly against it. It is possible to calculate electron-phonon coupling parameters within DFT and obtain an estimate the superconducting transition temperature, but such calculations are beyond the scope of this paper. The question of whether metallic  $AlH_3$  is a superconductor can only be answered by experiment.

## V. STABILITY AGAINST DEHYDRIDATION

Our structural search indicates the  $Pm\bar{3}n$  phase of  $AlH_3$  to be the most stable of this stoichiometry for a substantial range of pressures above 73 GPa, but there is another important aspect of stability which must be investigated.  $AlH_3$  is thermodynamically unstable with respect to decomposition

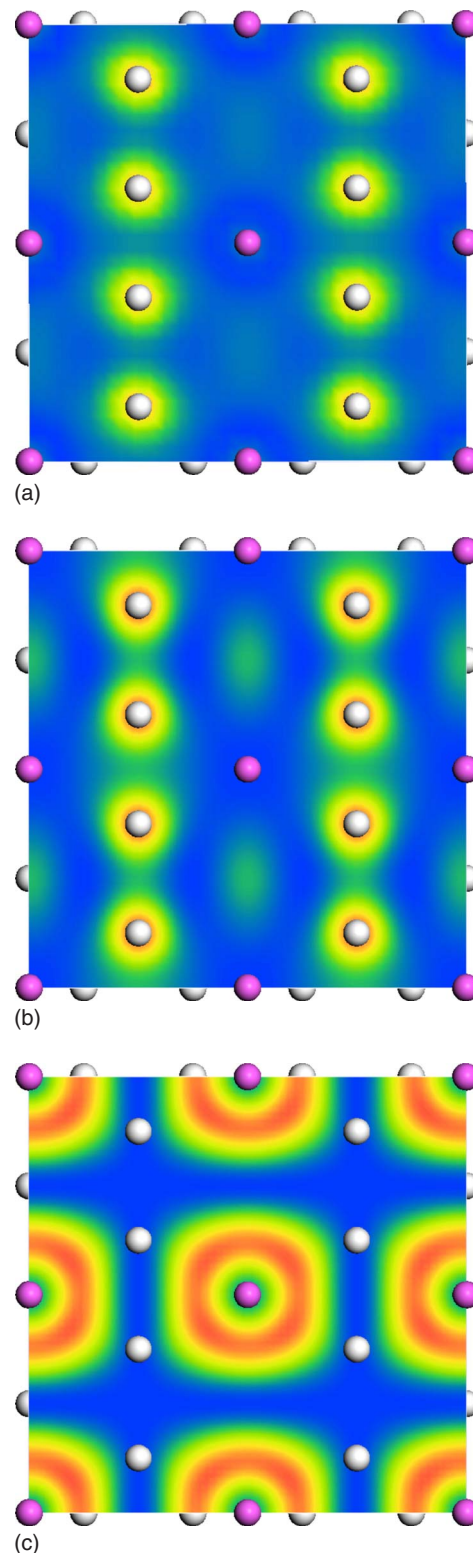


FIG. 6. (Color online) Charge density slices for the  $Pm\bar{3}n$  phase at 80 GPa, with the H atoms shown as light spheres and the Al atoms as dark spheres. Top: total valence charge density. Middle: charge density from the unoccupied highest-energy H-derived state at the  $M$  point (thick line in Fig. 4 at 0.6 eV). Bottom: charge density from the Al-derived occupied state at the  $R$  point (thin line in Fig. 4 at an energy of  $-0.9$  eV).

to its elements at STP,<sup>24</sup> and it releases H<sub>2</sub> molecules under moderate heating. Within PBE-GGA,  $R\bar{3}c$  is calculated to be unstable to decomposition to Al and H<sub>2</sub> by 3 meV per formula unit at zero pressure, in qualitative agreement with experiment. It is therefore important to investigate the stability of AlH<sub>3</sub> phases under pressure against dehydrogenation (segregation into AlH<sub>(3-x)</sub> and H<sub>2</sub>). We searched for the most stable high pressure (100 GPa) structures of AlH and AlH<sub>2</sub>, while for pure Al we took the face-centered cubic structure, and the  $Pa\bar{3}$  structure for H<sub>2</sub> (which models phase I of solid hydrogen).<sup>17</sup> We then calculated the enthalpies of these structures as a function of pressure. Combining these data with our results for AlH<sub>3</sub> (Fig. 1), we determined that the  $Pnma$  and  $Pm\bar{3}n$  phases are stable against dehydrogenation.

## VI. CONCLUSIONS

We have searched for high-pressure phases of AlH<sub>3</sub> using first-principles DFT methods. We predict a transition to an insulating layered  $Pnma$  phase at 34 GPa, followed by a transition to a metallic  $Pm\bar{3}n$  phase at pressures above

73 GPa. This pressure is comfortably within reach of diamond anvil cells. The very-high-symmetry  $Pm\bar{3}n$  structure consists of a body-centered cubic array of Al atoms and chains of metallic H atoms, and it has the same symmetry as the superconductor Nb<sub>3</sub>Sn (niobium stannide). The valence-conduction band overlap in this structure is substantial in both the PBE-GGA theory, which tends to underestimate band gaps, and in the sX-LDA approach, which generally gives band gaps in good agreement with experiment for *sp*-bonded systems. The  $Pm\bar{3}n$  structure has a high Debye temperature of about 2700 K at 80 GPa, which would tend to favor superconductivity, but the total density of electronic states at the Fermi energy is not very large, which strongly militates against it. The question of whether metallic AlH<sub>3</sub> is a superconductor can only be answered by experiment. We have found that the application of pressure tends to stabilize AlH<sub>3</sub> against dehydrogenation, and that the  $Pnma$  and  $Pm\bar{3}n$  phases are stable against such processes in their calculated ranges of stability. This suggests that the metallic  $Pm\bar{3}n$  phase could readily be formed in high-pressure experiments.

<sup>1</sup>G. Sandroek, J. Reilly, J. Graetz, W.-M. Zhou, J. Johnson, and J. Wegrzyn, *Appl. Phys. A* **80**, 687 (2005).

<sup>2</sup>T. Bazyn, R. Eyer, H. Krier, and N. Glumac, *J. Propul. Power* **20**, 427 (2004).

<sup>3</sup>J. Bardeen, L. N. Cooper, and J. R. Schrieffer, *Phys. Rev.* **108**, 1175 (1957).

<sup>4</sup>N. W. Ashcroft, *Phys. Rev. Lett.* **92**, 187002 (2004).

<sup>5</sup>J. Feng, W. Grochala, T. Jaron, R. Hoffmann, A. Bergara, and N. W. Ashcroft, *Phys. Rev. Lett.* **96**, 017006 (2006).

<sup>6</sup>C. J. Pickard and R. J. Needs, *Phys. Rev. Lett.* **97**, 045504 (2006).

<sup>7</sup>Y. Yao, J. S. Tse, Y. Ma, and K. Tanaka, *Europhys. Lett.* **78**, 37003 (2007).

<sup>8</sup>L. Sun, A. L. Ruoff, C.-S. Zha, and G. Stupian, *J. Phys.: Condens. Matter* **18**, 8573 (2006).

<sup>9</sup>M. Martinez-Canales, A. Bergara, J. Feng, and W. Grochala, *J. Phys. Chem. Solids* **67**, 2095 (2006).

<sup>10</sup>J. S. Tse, Y. Yao, and K. Tanaka, *Phys. Rev. Lett.* **98**, 117004 (2007).

<sup>11</sup>H. W. Brinks, A. Istad-Lem, and B. C. Hauback, *J. Phys. Chem. B* **110**, 25833 (2006).

<sup>12</sup>H. W. Brinks, W. Langley, C. M. Jensen, J. Graetz, J. J. Reilly, and B. C. Hauback, *J. Alloys Compd.* **443**, 180 (2007).

<sup>13</sup>H. W. Brinks, C. Brown, C. M. Jensen, J. Graetz, J. J. Reilly, and B. C. Hauback, *J. Alloys Compd.* **441**, 364 (2007).

<sup>14</sup>X. Z. Ke, A. Kuwabara, and I. Tanaka, *Phys. Rev. B* **71**, 184107 (2005).

<sup>15</sup>J. Graetz, S. Chaudhuri, Y. Lee, T. Vogt, J. T. Muckerman, and J. Reilly, *Phys. Rev. B* **74**, 214114 (2006).

<sup>16</sup>G. Csányi, C. J. Pickard, B. D. Simons, and R. J. Needs, *Phys. Rev. B* **75**, 085432 (2007).

<sup>17</sup>C. J. Pickard and R. J. Needs, *Nat. Phys.* **3**, 473 (2007).

<sup>18</sup>S. J. Clark, M. D. Segall, C. J. Pickard, P. J. Hasnip, M. I. J. Probert, K. Refson, and M. C. Payne, *Z. Kristallogr.* **220**, 567 (2005).

<sup>19</sup>J. P. Perdew, K. Burke, and M. Ernzerhof, *Phys. Rev. Lett.* **77**, 3865 (1996).

<sup>20</sup>D. Vanderbilt, *Phys. Rev. B* **41**, 7892 (1990).

<sup>21</sup>G. Onida, L. Reining, and A. Rubio, *Rev. Mod. Phys.* **74**, 601 (2002).

<sup>22</sup>M. J. van Setten, V. A. Popa, G. A. de Wijs, and G. Brocks, *Phys. Rev. B* **75**, 035204 (2007).

<sup>23</sup>M. C. Gibson, S. J. Clark, S. Brand, and R. A. Abram, *AIP Conf. Proc.* **772**, 1125 (2005).

<sup>24</sup>G. C. Sinke, L. C. Walker, F. L. Oetting, and D. R. Stull, *J. Chem. Phys.* **47**, 2759 (1967).